Proceedings of Ninth World Conference on Earthquake Engineering
August 2-9, 1988, Tokyo-Kyoto, JAPAN (Vol.IV)

6-1-13

PSEUDO-DYNAMIC TEST OF R/C MODELS CONSISTING OF DUCTILE AND BRITTLE COLUMN

Manabu YOSHIMURA[1] and Hideo TSUKAGOSHI[2]

1 Department of Architecture, Faculty of Engineering,
Tokyo Metropolitan University, Setagaya-ku, Tokyo, Japan
2 Technical Research Institute, Shimizu Construction Company,
Koto-ku, Tokyo, Japan

SUMMARY

Reinforced concrete model specimens consisting of columns with various ductility were tested by means of 'Pseudo-Dynamic' test method to examine the effect of column ductility on overall responses of the specimens to earthquake motions. The experiments confirmed that the specimen with brittle member underwent more damage and response displacement than the one without such member. Nonlinear response analysis conducted for the former case revealed the importance of properly estimating hysteresis damping in an unstable region of brittle member.

INTRODUCTION

There have been a number of tests on reinforced concrete frames and many informations have been derived from these studies. However, the past tests were almost limited to those on ductile frames and few attention have been paid to brittle frames. In the meanwhile, actual reinforced concrete building construction is in general not composed of ductile members alone but usually include some brittle members. And to clarify seismic behavior of such usual buildings, an attempt is indispensable to experimentally examine inelastic response of frames including brittle members to earthquake motions.

This paper is intended to present Pseudo-Dynamic (PD) test (Refs.1,2) of reinforced concrete model specimens consisting of ductile and brittle members. Discussions made herein are mainly concerned with the responses of the specimens after failure of the brittle member.

EXPERIMENTS

Model Specimens Dimensions and reinforcement arrangement of model specimens are shown in Figs.1 and 2. The specimens, designated as NO1, NO2 and NO3, were uniform in dimensions and consisted of column being 20cm wide by 20cm deep (hereafter referred to as column or C), broad column being 10cm by 40cm (referred to as wall-column or WC) and rigid girders connecting them. Clear height of the two vertical components was 100cm. The columns being uniform even in reinforcement arrangement, were designed so that a failure mode would be flexure. On the other hand, the wall-columns were designed to be identical in vertical reinforcement but different in horizontal reinforcement to result in various failure modes; flexure (NO1), flexural-shear (NO2) and shear (NO3).

Three-component load cell was incorporated in the column at midheight to measure shear and axial forces and moment. Placing the load cell at that location forced the specimens to be cast in two stages; firstly bottom girder and bottom half of the column were cast and secondly the remaining portions were constructed. Mechanical properties of concrete and reinforcement are listed in Table 1, in which alphabet D and numerals after this denote deformed bar and bar diameter in milimeter, respectively.

Loading Loading setup is shown in Fig.1. Vertical loads were applied by two vertical actuators placed at the sides of the specimen. For Specimen NO1, they were controled in such manner that the weight of L-shaped loading beam might be canceled, in other words, the specimen might be subjected to axial load only due to its own weight (1.6t for each vertical component). For NO2 and NO3, each vertical component was subjected to axial load of 5.6t including the specimen weight. Under constant axial load, the specimens were laterally loaded by horizontal actuator. Lateral loads were applied at midheight of the specimen.

Internal forces produced in the specimen due to lateral load were computed for elastic range (Fig.3). For both column and wall-column, computed end moments were almost the same in the magnitude and direction, and computed axial forces were negligibly small. Such results were because lateral load was applied at midheight of the specimen and the girders were stiff enough to be deemed rigid. Note that the wall-column was computed to carry 76.2% of the story shear.

Pseudo-Dynamic (PD) Test Computed horizontal strength and story stiffness of the specimens are shown in Table 2, in which weight assumed in the PD test and resulting base-shear coefficient (Ky in the figure) and period are also tabulated. In the PD test, viscous damping was ignored and the 1940 EL CENTRO NS record with normalized peak acceleration of 0.118g (Fig.4) was used as an input motion. Note that the level of peak acceleration was selected to be nearly identical to the base-shear coefficients.

The PD test was conducted during the steps corresponding to about seven seconds of the input motion except Specimen NO2, for which the PD test was stopped at about 4.5 seconds due to the disorder of displacement transducer used to control the test. After the PD test, additional Static-Loading (SL) test was performed to induce more damages in the specimens.

TEST RESULTS AND DISCUSSION

Lateral Load-Deflection Relations Lateral load - deflection (story shear - story drift) relations obtained from the PD test and SL test are illustrated in Fig.5 for each specimen. And envelopes of these relations are compared in Fig.6. Results of each specimen are stated below;

1) NO1 During the PD test with maximum story drift of 1.5% (by clear height), the specimen behaved in a very favorable manner. And it maintained sufficient ductility even at 5% story drift in the SL test. Such excellent behavior of this specimen was due to the fact that failure modes of the two vertical components were both flexure.

2) NO2 During the PD test with maximum story drift of 1.06%, the specimen showed stable behavior. However, at 1.5% story drift in the SL test (Point A in Fig.5) shear failure started to occur in the wall-column leading to strength decay.

3) NO3 At about 1.0% story drift in the PD test (Point A in Fig.5), shear failure occurred in the wall-column and such early brittle failure caused maximum story drift to reach as much as 2.11%. In the SL test damage and strength decay of the specimen increased further.

Observed maximum story shear exceeded by 20% to 40% the computed strength shown in Table 2. Possible sources for such increase in strength were strain hardening of main bars and inadequacy of the equation (Ref.3) used in computing shear strength.

Crack Formation of Wall-Column Crack formation of the wall-columns at 1.0% story drift is compared in Fig.7 for Specimen's NO1 and NO3. Wide shear crack formed in NO3 while such critical crack was not observed in NO1.

Behavior of Column and Wall-Column The relations of shear force carried by each vertical component and story drift observed in the PD test are shown in Fig.8 for Specimen NO3, in which column shear was obtained from the reading of the load cell and wall-column shear was derived by subtracting column shear from story shear. The wall-column showed significant hysteresis deterioration typical to shear failure while the column did not show such response. Since the levels of story drift at which the two vertical components reached peak loads were not identical, maximum story shear (16.6t) was less than the sum of their peak loads (17.6t).

The changes of the percentage of wall-column shear to story shear with respect to story drift are plotted in Fig.9 for the three specimens. For NO1 the percentage of wall-column shear was found to be high and nearly constant irrespective of the level of story drift. For the other specimens this percentage was observed to be high at small drift level but drop suddenly at certan drift levels; 1.5% for NO2 and 1.0% for NO3. Such drift levels apparently corresponded to the onset of shear failure of the wall-column. Note that the value of this percentage at small drift level was fairly close to the value computed for elastic range (76.2%).

Flexural and Shear Deformation of Wall-Column Average curvatures of the vertical components along height were measured, as illustrated in Fig.10. Based on such measurement flexural deformation of the wall-column was estimated by integrating average curvatures along height. Then shear deformation was computed as a difference of story drift and flexural deformation. The relations of these deformations and wall-column shear are shown in Fig.11 for NO2 and NO3. Results of each specimen are stated below;

1) NO2 Before Point A in Fig.11, flexural deformation was predominant. However, afer this point at which shear failure started to occur, shear deformation drastically increased while flexural deformation decreased.

2) NO3 Even before Point A in Fig.11, shear deformation was comparable to flexural deformation, and after this point corresponding to the onset of shear failure, the former overwhelmed the latter.

RESPONSE ANALYSIS OF SPECIMEN NO3

Method of Analysis Inelastic response of Specimen NO3 was analysed. In the analysis the specimen was idealized as one-bay and one-story frame with rigid girders, and two different hysteresis models, Degrading Tri-Linear model and Origin-Oriented model(Ref.4) were used to represent inelastic behavior of the column and wall-column, respectively. Backbone curves of the hysteresis models were analytically established except shear strength and post-failure negative slope of the wall-column, which were determined in reference to the test results.

Results of Analysis Observed and computed relations of story, column and wall-column shear and story drift are compared in Fig.8. Observed and computed response waveforms of story drift are also compared in Fig.12. Until the point of maximum story drift in the positive direction at about 5.3sec (Point C in

Fig.12), the computed response fairly matched with the observed. However, beyond this point the computed story drift was found to become much larger than the observed. Such discrepancy between the observed and computed responses is believed to be due to the underestimate of area of the hysteresis loops in the Origin-Oriented model (Fig.8). The underestimated hysteresis loops in the analysis caused less hysteretic damping, which resulted in larger story drift.

CONCLUSION

Major findings from the studies are summarized as follows;

1) Pseudo-Dynamic test method can experimentally simulate inelastic response of a brittle frame to earthquake motions even over an unstable region,

2) A brittle frame undergoes more damage and response displacement than a ductile frame with same strength against the same input ground motions, and

3) To analytically reproduce inelastic response of a brittle frame, proper estimation of hysteretic damping in an unstable region is important.

REFERENCES

1)Takanashi, K. and Nakashima, M., "Japanese Activities on On-Line Testing", Journal of the Engineering Mechanics, ASCE, Vol.113, July 1987, pp. 1014-1032

2)Mahin, S.A. and Shing, P.B., "Pseudodynamic Method for Seismic Testing", Journal of the Structural Engineering, ASCE, Vol. 111, No.1, July 1985, pp.1482-1503

3)"AIJ Standard for Structural Calculation of Reinforced Concrete Structures", Japan Architectural Institute, 1982

4)Hirosawa, M., Kitagawa, Y. et al., "Analysis in Damage of the Namioka Town Hospital Building During the 1983 Nihonkai-Chubu Earthquake and Retrofit Design of the Building", BRI Research Paper, Building Research Institute, Ministry of Construction, Japan, 1985

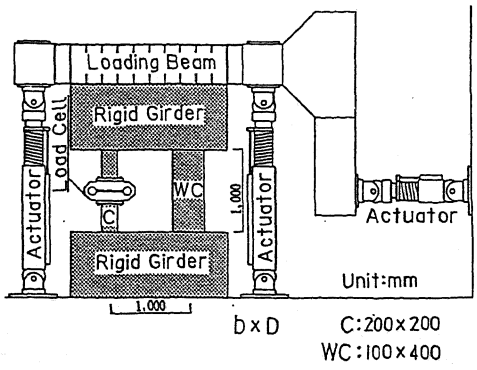

Fig.1 Model Specimen and Loading Setup

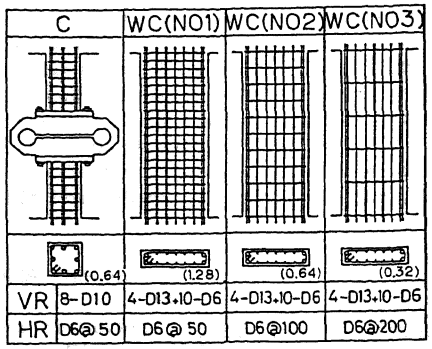

Fig.2 Reinforcement Arrangement

Table 1 Mechanical Properties of Material

	Fc			σy		
	1st	2nd	Av	D6	D10	D13
NO1	320	385	353	3500	3580	3620
NO2,NO3	195	183	189	3360	3940	3970

Fc : Compressive Strength of Concrete
σy : Yield Stress of Reinf. Unit:Kg/cm^2

Table 2 Computed Horizontal Strength and Story Stiffness

	Q(t)	W(t)	KY=Q/W	KG	KY/KG	ST(t/cm)	T(sec)
NO1	13.7	114.	.120	.118	1.02	171	.164
NO2	14.4	114.	.126	.118	1.07	125	.192
NO3	13.2	114.	.116	.118	.983	125	.192

Q:Horizontal Strength ST:Story Stiffness
W:Assumed Weight T:Period
KG:Peak Acc. of Input Motion(g)

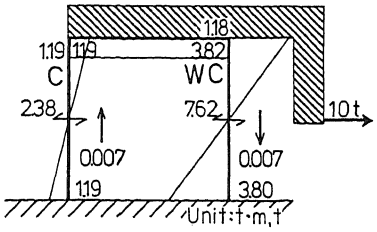

Fig.3 Internal Forces Due to Lateral Load

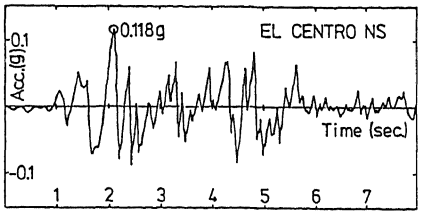

Fig.4 EL CENTRO NS Record

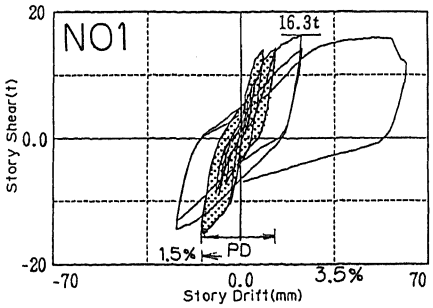

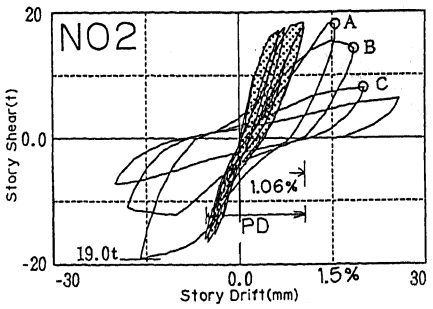

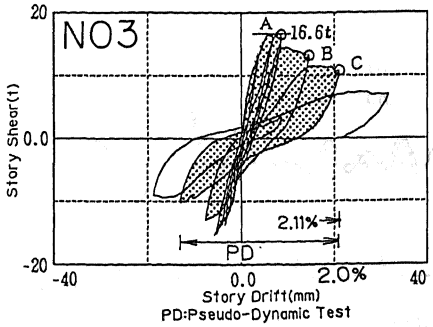

Fig.5 Story Shear-Story Drift Relations

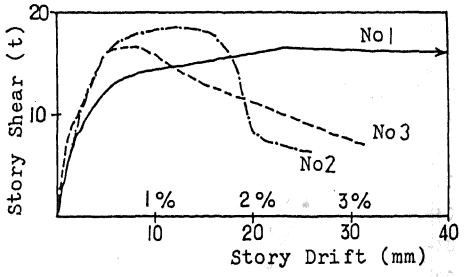

Fig.6 Comparison of Envelopes

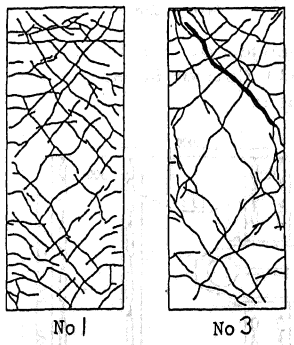

Fig.7 Crack Formation of Wall-Column

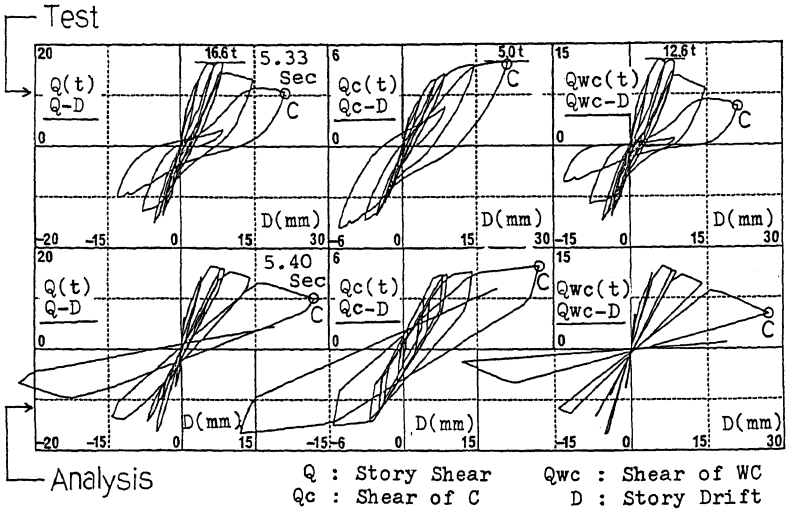

Fig.8 Observed and Computed Relations of Story, Column and Wall-Column Shear and Story Drift for NO3

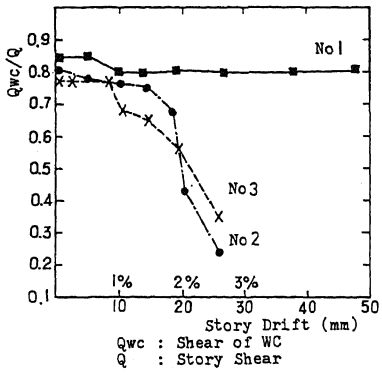

Fig.9 Changes of Percentage of Wall-Column Shear to Story Shear

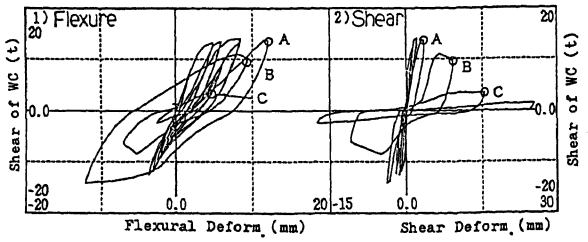

a) NO2

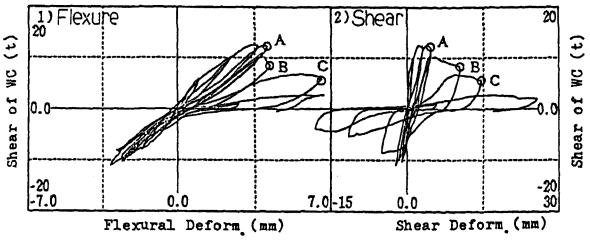

b) NO3

Fig.11 Relations of Flexural and Shear Deformations and Shear for Wall-Column

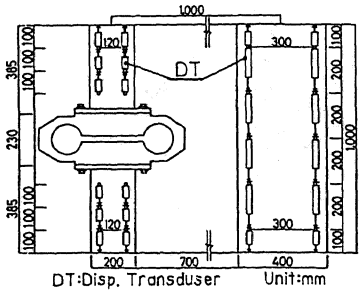

Fig.10 Measurement of Average Curvatures

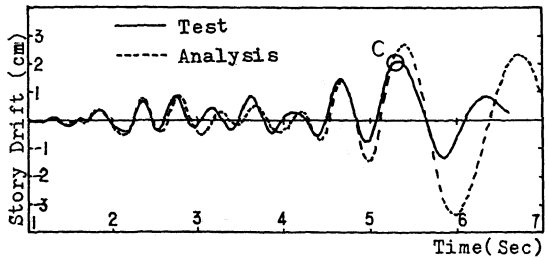

Fig.12 Observed and Computed Response Waveforms of Story Drift for NO3